Astron. Astrophys. 319, 201–210 (1997)

ASTRONOMY
AND
ASTROPHYSICS

X-ray properties of symbiotic stars

II. Systems with colliding winds⋆

Urs Mürset[1], **Burkhard Wolff**[2], **and Stefan Jordan**[2]

[1] Institut für Astronomie, ETH Zentrum, CH-8092 Zürich, Switzerland (muerset@astro.phys.ethz.ch)
[2] Institut für Astronomie und Astrophysik, Universität Kiel, D-24098 Kiel, Germany (wolff/jordan@astrophysik.uni-kiel.d400.de)

Received 14 June 1996 / Accepted 24 July 1996

Abstract. 60% of the known galactic symbiotic stars are sufficiently X-ray bright to be detected in pointed ROSAT PSPC observations. We present observations of 16 symbiotic stars. We encounter three classes of pulse height distibutions: α) supersoft emission from the atmosphere of the hot star, β) emission from an optically thin plasma with a temperature of a few 10^6 K, and γ) even harder emission, as from an accreting neutron star. In the present Paper we analyze the objects of type β in more detail. We find plasma temperatures ranging from $3 \cdot 10^6$ K to $15 \cdot 10^6$ K and luminosities from $2 \cdot 10^{-4}$ $L_\odot$ to 0.4 $L_\odot$.

Key words: binaries: symbiotic – stars: individual: EG And – stars: individual: PU Vul – stars: individual: Hen 1591 – stars: mass-loss – X-rays: stars

1. Introduction

Symbiotic stars are interacting binaries consisting of a red giant and a very hot, probably degenerate companion. Already the optical spectrum is peculiar, showing high ionization emission lines, often with complex profiles. But nearly every spectral range that has been opened for astronomy brought new and surprising observational facts. The latest step of that kind is the advent of X-ray telescopes, in particular of the ROSAT satellite.

Details about the hot star and about the interaction mechanisms are poorly known: Where does the hot star get its energy from? Is there (constant or episodic) mass transfer? Where are the emission lines produced? In the "standard model" of e.g. Seaquist et al. (1984), Taylor & Seaquist (1984), and Nussbaumer & Vogel (1987) the nebula is assumed to be generated in the wind from the cool giant. A section of this wind is photo–ionized by the hot star but not otherwise disturbed. The situation is basically symmetric about the axis connecting the two binary components. The hot star may spherically accrete some matter from this nebula. The energy source of the hot star is either gravitational, or the accreted matter burns constantly or episodically at the surface.

However, at least in some cases, the hot star seems to be losing mass itself, rather than accreting (e.g. Thackeray & Webster 1974, Penston & Allen 1985, Vogel 1993, Vogel & Nussbaumer 1994, Nussbaumer et al. 1995), but it is not clear how frequent this phenomenon is and what the parameters of the winds from the hot stars are. Since symbiotic stars are sometimes suspected to be the progenitors of type Ia supernovae (e.g. Munari & Renzini 1992) it is of broad interest whether the degenerate star effectively gains or loses mass in the course of time.

A wind from the hot star completely changes our expectation of the structure of the nebula. The nebula will strongly differ from the model mentioned above (e.g. Kwok et al. 1984, Wallerstein et al. 1984, Girard & Willson 1987). Hydrodynamical modelling of colliding winds in symbiotic systems (Nussbaumer & Walder 1993, Walder 1995a,b) predict a warped, thin shell where the two winds collide and where temperatures up to $T_{\rm plasma} \sim 3 \cdot 10^7$ K have to be expected.

Unfortunately, the wind collision is not easily observed, but theory predicts X-ray emission (e.g. Willson et al. 1984, Walder & Vogel 1993), so that indirect evidence for wind collision can be obtained. For the first time we have the opportunity to determine the frequency of the phenomenon, to measure the energetics involved and to test the hydrodynamical models.

We have already analyzed ROSAT observations of AG Peg (Mürset et al. 1995). In the present Paper, we report on the results of a systematic archive search for pointed ROSAT observations of symbiotic stars. In Sect. 2 we present the data, in Sect. 3 we analyze those objects with a hot plasma component, and in Sect. 4 we discuss the results. – Preliminary results on our search were presented in Mürset et al. (1996b; Paper I). We plan to investigate the photospheric X-ray sources in a forthcoming Paper III.

Send offprint requests to: U. Mürset

⋆ Based on data collected with the ROSAT satellite

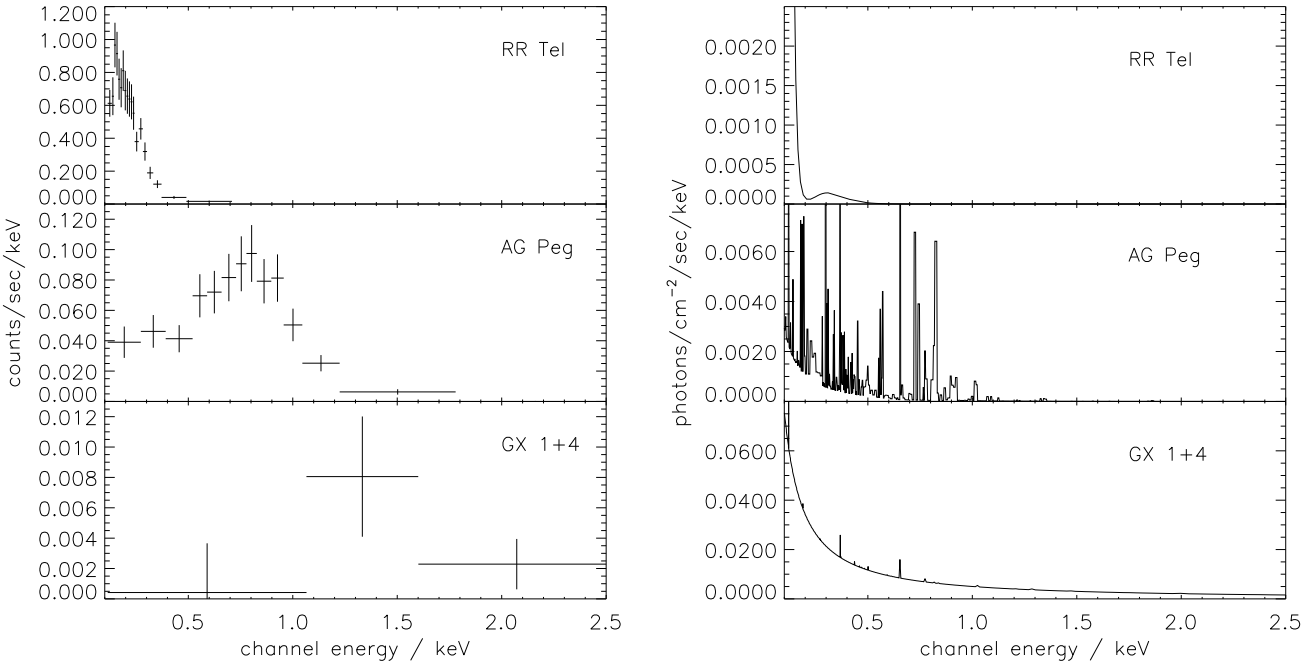

Fig. 1. The three types of X-ray spectra of symbiotic stars (see text). RR Tel is of type α, AG Peg of type β, and GX1+4 of type γ. **Left:** observed pulse height distributions. Note that these data are not corrected for the instrumental response which varies strongly over the covered energy interval. **Right:** Models for the objects that fit the observations after attenuation by interstallar matter and convolution with the PSPC response matrix. The α-type is fitted with a NLTE model atmosphere (Jordan et al. 1994), the β-type with a 0.3 keV Raymond–Smith type plasma (Mürset et al. 1995), and Predehl et al. (1995) suggested a high energy plasma (50 keV) as the source of the γ type emission of GX1+4.

2. Data from the ROSAT archive

We searched in the ROSAT archive (January 1996) for frames covering the positions of symbiotic stars. The search included the catalogue by Allen (1984, "possible" objects included), the LMC and SMC objects listed in Mürset et al. (1996a), and, in addition, the following confirmed or suspected symbiotics: MWC 560 (Michalitsianos et al. 1991), S32 and S190 (Downes & Keyes 1988), N19 (Morgan 1996), SMP94 (Dopita et al. 1985; Meatheringham & Dopita 1991), RAW1691 (Rebeirot et al. 1993). We excluded the recurrent novae RS Oph (see Orio 1993 instead) and T CrB. In total, we searched for 154 objects. Table 1 gives a list of the objects found in fields of pointed observations. In many cases the symbiotic stars are not the very target of the observation, but incidently in the 2° PSPC field of another object.

The pulse height distributions of the symbiotic stars were extracted using the EXSAS software package (Zimmermann et al. 1994). The counts were binned until a signal-to-noise ratio of 5 (GX 1+4 and PU Vul: 4) was achieved in each bin. Figs. 2 to 4 display the resulting pulse height distributions. The count rates obtained by integration over all energy channels are given in Table 1.

3. Analysis

3.1. Three classes

The extracted pulse height distributions can clearly be divided into three distinct groups (see Fig. 1):

- α: supersoft distributions, i.e. essentially all counts below $h\nu \approx$ 0.4 keV. The observations are collected in Fig. 2.
- β: objects with harder pulse height distributions that typically peak at about 0.8 keV. The objects of this type are shown in Fig. 3.
- γ: relatively hard X-ray sources like GX1+4 (Fig. 4). In fact, GX1+4 has the hardest spectrum of all known X-ray binaries (Predehl et al. 1995).

A weak, superimposed X-ray component of type β was detected in RR Tel which is an object of type α (Jordan et al. 1994). From this fact we learn that the different emission sources do not necessarily exclude each other mutually. The classification of an object just mirrors the relative strengths of the components.

3.2. A one-point plasma model

In the following we try to model the pulse height distributions of type β. For the case of the strongest β-type source, AG Peg, Mürset et al. (1995) showed that it can be reproduced with the emission of a very hot, optically thin plasma. Such a plasma could be prduced by colliding winds as mentioned in the introduction, but also in accretion shocks or in an accretion disk. We

Table 1. Symbiotics in the ROSAT pointed observations archive. The upper part of the table lists detections, the lower part upper limits for the count rates of non-detections. The observations for AG Dra are described in more detail in Greiner et al. (1996).

Object	Date	Observation	Exposure time [s]	Integrated count rate [10^{-2} s^{-1}]
EG And	1991, July 27 – 28	WG600068P	30 594	0.8 ± 0.3
SMC 3	1991, Oct 9 – 1992 Apr 25	WG600196P	24 031	20.4 ± 0.4
Ln 358	1992, Oct 2 – Nov 11	WG201094P	64 695	2.9 ± 0.2
RX Pup	1993, April 14 – June 8	US300187P	3 238	6.0 ± 0.6
AG Dra	1992, April – 1993, May	several	1 339 – 2 525	$92 \ldots 114 \pm 3$
Draco C–1	1992, April 1	WG200724P	5 375	5.3 ± 0.6
GX1+4	1993, Sept 18	WG180030P	2 316	0.6 ± 0.4
Hen 1591	1993, Sept 10	WG400396P	2 016	1.4 ± 0.6
CH Cyg	1992, March 28/29	US900159	8 272	37.2 ± 0.9
HM Sge	1992, Nov 1 – 3	WG201100P	6 734	4.5 ± 0.4
V1016 Cyg	1992, Nov 18 – 19	WG201099P	15 950	1.2 ± 0.3
RR Tel	1992, April 17 – 23	WG200581P	5 844	18.3 ± 0.8
PU Vul	1992, Nov 10 – 12	US300182P	27 057	0.4 ± 0.1
CD–43.14304	1993, April 8 – Oct 29	WG201091P,P-1	13 726	9.1 ± 0.4
AG Peg	1993, June 9/10	US300186P	6 004	6.7 ± 0.5
Z And	1993, Jan 5 – 9	US300189P	9 865	0.3 ± 0.2
R Aqr	1992, Dec 20 – 21	WG701205P	14 434	4.1 ± 0.3
SMC2	1992, Oct 2 – Nov 11	WG201094P	64 695	< 0.04
RAW1691	1991, Oct 16 – 19	WG600197P	21 494	< 0.05
N19	1992, Apr 11 –14	WG500060P	4 022	< 0.12
N67	1990, Jul 9 – 10	CA140635P	1 540	< 0.11
Sanduleak's star	1993, Sep 24 – 30	WG201610P	7 848	< 0.21
MWC 560	1992, Apr 29 – 30	WG300132P	4 664	< 0.07
He2–38	1991, Dec 11 – 12	WG200715P	7 805	< 0.19
RW Hya	1992, Jan 30 – Feb 1	UK200445F (with Boron filter)	3 038	< 0.09
"	"	UK200445P (without filter)	1 007	< 0.30
Ap1–8	1993, March 31 – April 1	WG201093P	10 039	< 0.09
H2–38	"	"	"	< 0.06
Ap1–9	1993, March 30 – April 6	US300188P	9 980	< 0.02
AS281	"	"	"	< 0.02
AS296	1992, Mar 08 – Mar 23	US300107P	8 467	< 0.02
MWC 960	1993, April 9 – 14	US201022P	10 479	< 0.05

assume that this holds for all β-type objects. We restrict ourselves to a one point model with a single temperature. In view of the complex structures predicted by model calculations for colliding winds (Walder 1995a,b), this is a crude approximation. However, a model with a larger number of parameters is not appropriate for the present data, and according to our experience with AG Peg this approach is still suitable to derive the energetics of the phenomenon.

For the elemental composition of the emitting plasma we adopt solar abundances. In order to lower the number of fit parameters we assume a hydrogen column density, $N_{\rm H}$, as described in the next paragraph.

The free parameters for the model are the plasma temperature $T_{\rm plasma}$ and a factor A which is the emission measure, E.M., scaled by the distance, d:

$$A = \frac{\rm E.M.}{4\pi {\rm d}^2} = \frac{1}{4\pi d^2} \cdot \int N_{\rm e} \cdot N_{\rm H^+} \, {\rm d}V \ . \qquad (1)$$

Table 2. Distances and interstellar extinctions employed in the analysis. The extinction towards RX Pup appears to be uncertain, we therefore allow for a certain range of values.

Object	d [kpc]	Reference	$E_{\rm B-V}$ [mag]	Reference
EG And	0.32	1	0.05	1
RX Pup	1.8	2	0.55 ± 0.15	3
HM Sge	2.9	1	0.65	1
V1016 Cyg	3.9	1	0.40	1
PU Vul	1.8	4	0.40	4

1) Mürset et al. (1991); 2) this Paper;
3) Ivison & Seaquist (1994), Allen & Wright (1988);
4) Vogel & Nussbaumer (1992)

With the EXSAS software package we calculated a grid of theoretical X-ray fluxes (according to Raymond & Smith 1977) for different temperatures of the hot, optically thin plasma. These

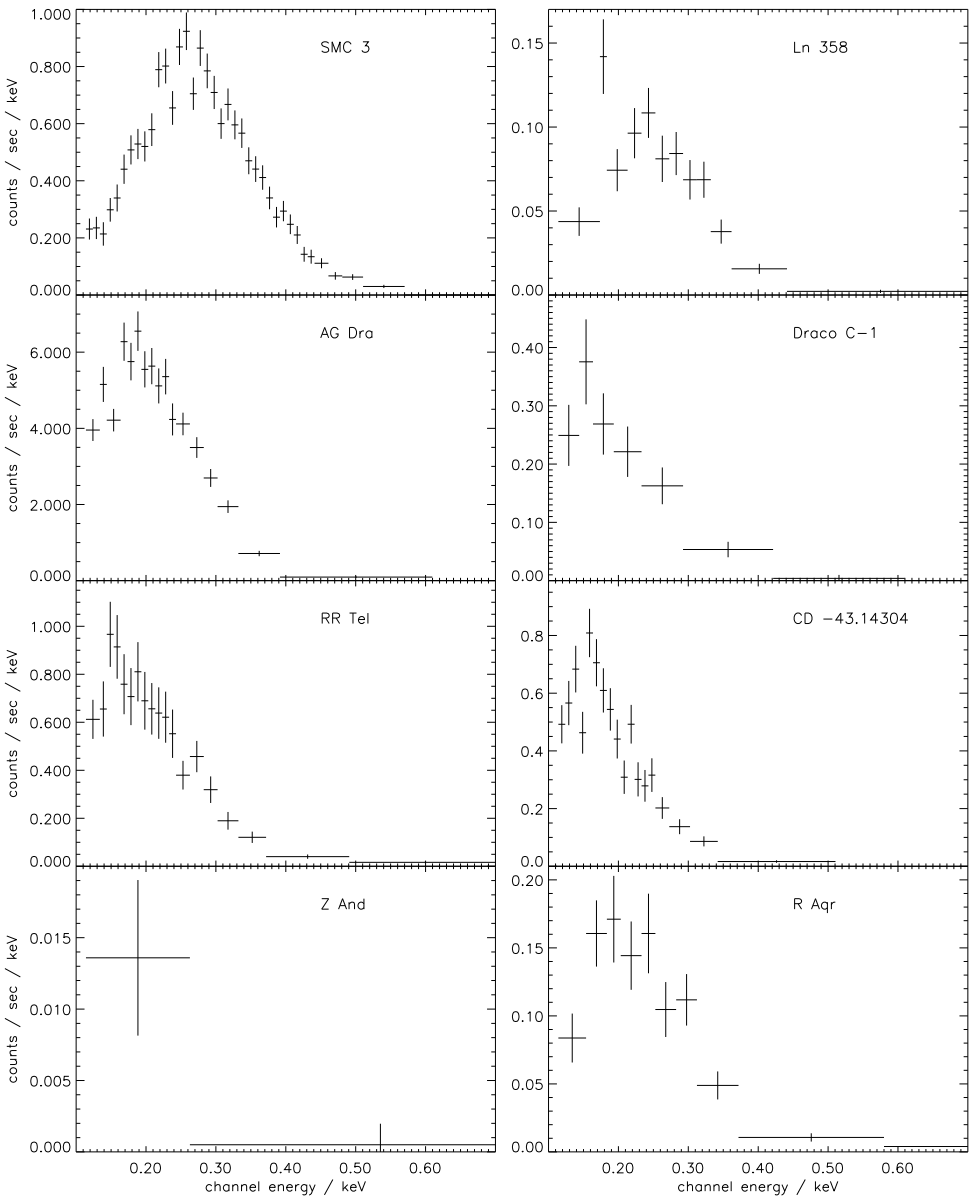

Fig. 2. Supersoft pulse height distributions of symbiotic stars (type α). It is probable that nearly all of the X-ray flux comes from the hot star's photospheres.

fluxes were converted to theoretical pulse height distributions, and a χ^2 analysis for $T_{\rm Plasma}$ and A was performed.

In order to derive the emission measures and the plasma luminosities we need the distances. Table 2 lists the adopted distances. The value for RX Pup was derived by us with the help of the period-luminosity–relation for mira variables; in the details, we follow the procedure of Mürset et al. (1991) for the distance of V1016 Cyg. No values are given for AG Peg (for which we adopt the results of Mürset et al. 1995) and CH Cyg (no solution).

3.3. The column density

In most cases, the quality of the data does not allow to leave $N_{\rm H}$ as a free parameter. We are, thus, forced to make assumptions for the column densities. A lower limit for $N_{\rm H}$ is derived from the foreground interstellar extinction. Published values for the extinction, $E_{\rm (B-V)}$, are collected in Table 2. They are converted into $N_{\rm H}$ values with the formula from Groenewegen & Lamers (1989).

An additional contribution to $N_{\rm H}$ has to be considered from the circumstellar gas lost by the cool star. The situation is probably different for s-type than for the d-type systems (RX Pup, V1016 Cyg, and HM Sge) because they strongly differ in mass loss and, consequently, in the column density of the attenuating circumstellar matter. An upper limit for $N_{\rm H}$ can be derived in some cases from the attenuation of the radiation from the hot star: The shock region is fairly extended (Walder 1995b) and will not be eclipsed as strongly as the star.

s-types: The cool components are normal red giants with comparably moderate mass loss. The hydrogen column in front of the hot star in EG And was measured as a function of the orbital phase by Vogel (1991). The column density can be as

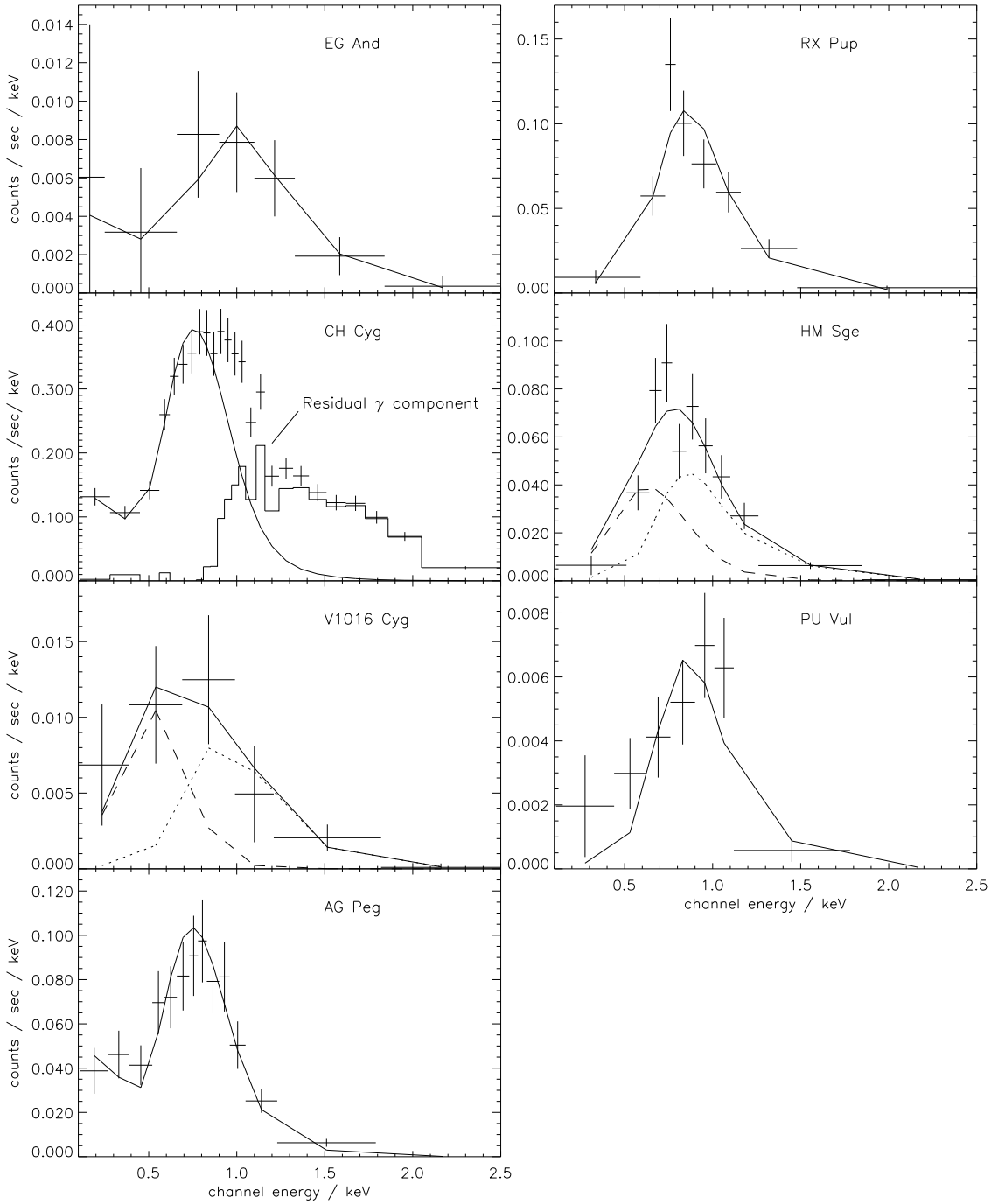

Fig. 3. PSPC pulse height distributions of seven symbiotic stars of type β. The fits were performed with one-temperature Raymond-Smith models (see Table 3 for the parameters). In the case of CH Cyg only the low energy part could be fitted; the residual "γ" component is indicated. For HM Sge and V1016 Cyg we also tested the influence of a hot component with 200 kK and 141 kK, respectively, with $N_{\rm H}$ choosen that the model fits the low energy part (long-dashed curve). The Raymond-Smith fit to the residuum is drawn as a dotted curve

large as 10^{25} cm^{-2} when the hot star shines through the entire wind, shortly before or after eclipse. It is, however, negligible at orbital phases far from eclipse. We therefore neglect the circumstellar absorption for the s-type objects which were all observed out of eclipse. For one of the s-type objects, AG Peg, the data are good enough to leave $N_{\rm H}$ as a free parameter. Mürset et al. (1995) found a total column density in agreement with the interstellar reddening.

d-types contain mira variables with long pulsation periods (580 d, 527 d, and 450 d respectively; Whitelock et al. 1983, Munari & Whitelock 1989, Taranova & Yudin 1983). Such objects suffer very strong mass loss; they are probably near the onset of the superwind phase (Schild 1989). Kenyon et

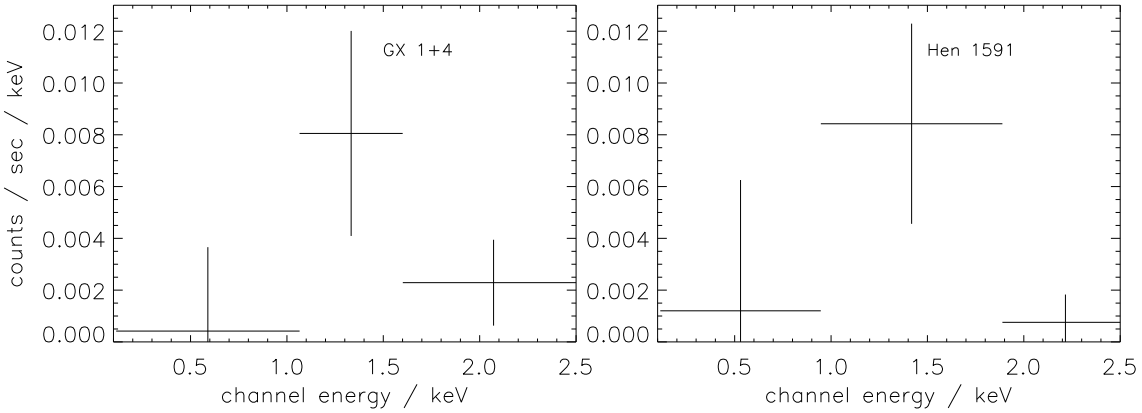

Fig. 4. Pulse height distributions of symbiotic stars of type γ.

al. (1988) estimated a mass loss rate of $\dot{M} \approx 10^{-5}$ $M_\odot$/yr for the objects in question. Temperature and luminosity of the hot stars in V1016 Cyg and HM Sge were determined by Mürset & Nussbaumer (1994). With only the foreground extinction, these hot stars would contribute much more to the low energy channels of the PSPC than observed. With a column density of $N_H \sim 10^{22}$ cm^{-2} the hot star would be strongly attenuated so as not to contribute anymore to the PSPC observations. We can exclude an even larger column density because it would show up through Rayleigh scattering in the UV which is not observed. 10^{22} cm^{-2} is therefore taken as an upper limit for N_H.

We decided to adopt the foreground column for all objects. In addition, we made test fits assuming much larger N_H for V1016 Cyg and HM Sge: i) $N_H = 10^{22}$ cm^{-2}; ii) N_H such that the contribution from the hot star fits to the pulse heights of the lowest energy channels.

4. Discussion

4.1. Abundance of X-ray symbiotics

Six of our objects were already detected with EINSTEIN or EXOSAT (Allen 1981, Anderson et al. 1981, Willson et al. 1984, Kwok & Leahy 1984, Piro et al. 1985, Viotti et al. 1987, Leahy & Taylor 1987, Viotti et al. 1995) while GX1+4 was observed with several other X-ray experiments (see e.g. Greenhill et al. 1993). In the ROSAT all-sky survey 17 objects from our search list were detected (Bickert et al. 1996). A total of 31 symbiotic stars are in the fields of pointed PSPC observations (cf. Table 5). In 17 cases the objects were detected. Considering only the galactic objects, we find that 14 out of 23, or about 60 % of the symbiotic stars are detected. Although the exposure times of the various observations are too arbitrary to serve for sound statistics, we think that this percentage qualifies symbiotics as X-ray bright stars. There is no significant difference in the detectability of s- and d-types. The detection rate is somewhat larger for high galactic latitudes: for $|b| > 20°$, 6 out of 7 observed galactic symbiotics are detected, but only 8 out of 16 for $|b| < 20°$. We attribute this to the influence of the interstellar extinction in the plane of the milky way. On the other hand, the two γ-types, whose high energy radiation is less affected by foreground absorption, are both conspicuously close to the direction towards the center of galaxy. The abundance of symbiotic novae is discussed in Sect. 4.5.

4.2. The three X-ray types

So far, the system of three X-ray types is a mere observational discovery. It becomes a meaningful classification scheme if it is related to physical parameters of the system. Indeed, a physical interpretation of the $\alpha/\beta/\gamma$–system appears well possible:

- α: a supersoft spectrum is expected from those symbiotic systems which contain particularly hot white dwarfs. In these cases the photospheres produce photons sufficiently hard ($h\nu \approx 0.2$ keV) to leak into the ROSAT window. Jordan et al. (1994, 1996) successfully reproduced the pulse distribution of two α-type objects with hot model atmospheres.
- β: Three symbiotic stars that have been observed with HST high resolution spectroscopy (AG Peg: Nussbaumer et al. 1995; PU Vul: Nussbaumer & Vogel 1996; EG And: Schmutz et al., in preparation) exhibit broad profiles in the UV resonance lines that are characteristic for a strong 1000 km/s wind. In the region where this wind crashes into the cool star or its wind, the gas will be heated to several 10^6 K and produce optically thin Raymond–Smith type X-Ray emission. Indeed, for the case of AG Peg the data are in accordance with the result of a hydrodynamic calculation (Mürset et al. 1995). In this Paper we assume that β-type emission is due to hot, shocked gas. The β-types are probably objects where the hot star has a particularly strong mass loss. It is, however, also possible that shocks arise in an accretion flow.
- γ: GX1+4, which is one of the two γ–type objects, hosts a neutron star as hot component (e.g. Davidsen et al. 1977).

The $\alpha/\beta/\gamma$–classification, thus, mirrors basic properties (temperature, mass-loss, white dwarf/neutron star) of the hot star. This reminds us of the infrared classes s and d (Webster & Allen 1975) which mainly correspond to basic parameters of the cool star.

Table 3. Results: The classification of the detected systems is given in the fourth column. Columns 5 to 8 give the parameters of the plasma emission. ϕ is the orbital phase with ϕ = 0 when the cool star is in front. The quoted errors include 1 σ uncertainties around the best fits as well as the uncertainty in the formula of Groenewegen & Lamers (1989) used to derive $N_{\rm H}$. χ^2 gives the quality of the best fit.

Object	Date	ϕ	Type	$\log\left(\frac{T_{\rm Plasma}}{\rm K}\right)$	$\log\left(\frac{L_{\rm Plasma}}{\rm L_\odot}\right)$	$\log\left(\frac{E.M.}{\rm cm^{-3}}\right)$	χ^2 or Reference
EG And	July 1991	0.37	β	7.19 ± 0.15	-3.75 ± 0.21	52.79 ± 0.59	0.15
SMC 3	April 1992		α				
Ln 358	Oct/Nov 1992		α				
RX Pup	April – June 1993		β	6.87 ± 0.15	-0.92 ± 0.24	55.17 ± 0.25	1.1
AG Dra	1992 – 1993		α				
Draco C–1	April 1992		α				
GX1+4	Sept 1993		γ				
Hen 1591	Sept 1993		γ				
CH Cyg	March 1992	0.73	β	no satisfactory solution			
HM Sge	Nov 1992		β	6.63 ± 0.13	-0.36 ± 0.24	55.75 ± 0.30	1.5
V1016 Cyg	Nov 1992		β	6.59 ± 0.35	-1.03 ± 0.25	55.32 ± 0.60	1.4
RR Tel	April 1992		α	~ 6.5	~ -1.5	~ 54.7	a
PU Vul	Nov 1992	0.90	β	6.79 ± 0.25	-2.26 ± 0.28	53.89 ± 0.30	1.6
CD–43.14304	April 1993		α				
AG Peg	June 1993	0.89	β	6.5	-2	54.2	b
Z And	Jan 1993		α				
R Aqr	Dec 1992		α				

a: from Jordan et al. (1994); b: from Mürset et al. (1995); References for the orbital phases:
Vogel et al. (1992, EG And), Hinkle et al. (1993, CH Cyg), Nussbaumer & Vogel (1996, PU Vul), and Fernie (1985, AG Peg).

Table 4. Attempts to fit the pulse height distributions of HM Sge and V1016 Cyg with increased column densities.

Object	$N_{\rm H}$ [10^{21} cm^{-2}]	$\log\left(\frac{T_{\rm Plasma}}{\rm K}\right)$	$\log\left(\frac{L_{\rm Plasma}}{\rm L_\odot}\right)$	$\log\left(\frac{E.M.}{\rm cm^{-3}}\right)$	T^* [K]	R^* [R$_\odot$]
HM Sge	6.5	6.65 ± 0.25	-0.18	55.76 ± 0.52	200 000	0.08
	10	6.06 ± 0.05	+2.92	55.84 ± 0.54		
V1016 Cyg	1.9	7.01 ± 0.18	-1.33	54.68 ± 0.34	141 000	0.30
	10	6.04 ± 0.06	+2.72	< 56.4		

Out of the 16 detections, 7 are supersoft (type α), 7 of type β, and 2 are γ-types. For the milky way galaxy the ratio is 4 : 7 : 2, while all extragalactic objects are of type α. These figures possibly imply the following:

– β-type emission is not produced with count rates that would allow an extragalactic detection with ROSAT. α-type emission, in contrast, can reach high luminosities (e.g. SMC 3 which has the 3$^{\rm d}$ largest count rate of our sample, Jordan et al. 1996) while its detection depends crucially on the interstellar extinction, which is low towards the Magellanic Clouds.
– Adopting the galactic ratio as more significant, we find colliding winds in more than half of the detected objects. Furthermore, signs of mass loss from the hot star was found in the analysis of the two α-types RR Tel (Jordan et al. 1994) and SMC 3 (Jordan et al. 1996). We conclude that a large fraction of the symbiotic systems contains hot stars that lose mass. The question arises where these hot white dwarfs take their energy from if they do not accrete and/or burn accreted matter.
Munari & Renzini (1992) suspected the symbiotic systems to be the precursors of type Ia supernovae. However, for this scenario the white dwarfs would have to gain mass until they reach the Chandrasekhar limit. The more systems are found that lose mass instead of accreting the less plausible is this suggestion. One may speculate whether the hot star can accrete and lose mass at the same time on different parts of its surface.

4.3. X-ray luminosities and the efficiency of X-ray production

Table 3 lists the fit parameters derived for the plasma emission. The respective fits to the observations are shown in Fig. 3.

Table 4 shows the results of fits for HM Sge and V1016 Cyg with column densities larger than derived from the interstellar extinction. The first row of each object is the result of a two

Table 5. Search statistics

	galactic symbiotics			extragalactic symbiotics			symbiotic novae		total
IR-type	s	d	s+d	s	d	s+d	s	d	s+d
searched	110	29	139	11	4	15	5	3	154
observed	16	7	23	7	1	8	3	3	31
$\frac{\text{detected}}{\text{observed}}$ [%]	56	71	61	43	0	38	100	100	55
$\frac{\text{type } \alpha}{\text{detected}}$ [%]	33	40	36	100	–	100	33	33	47
$\frac{\text{type } \beta}{\text{detected}}$ [%]	44	60	50	0	–	0	67	67	41
$\frac{\text{type } \gamma}{\text{detected}}$ [%]	22	0	14	0	–	0	0	0	12

Table 6. Comparing wind and X-ray parameters. The data for AG Peg are from Schmutz (1996) and Mürset et al. (1995), the data for EG And from Schmutz et al. (in preparation), and the data for SMC 3 are from Jordan et al. (1996).

Parameter	AG Peg	EG And	SMC 3
Terminal velocity v_∞ [km/s]	950	900	?
Mass loss $\log(\dot{M})$ [$M_\odot$/yr]	-6.7	-8.3	≈ -5
Kinetic power $\frac{1}{2}\dot{M}v_\infty^2$ [$L_\odot$]	16	0.3	$\sim 10^3$
X-ray luminosity L_X [$L_\odot$]	0.01	0.0002	$\lesssim 3$
Efficiency [‰]	0.6	0.7	$\lesssim 3$

component fit. The first component is a model atmosphere appropriate for the hot star. It is of the same type as the atmosphere model used for RR Tel by Jordan et al. (1994). N_H is adjusted in a way that the hot star's emission reproduces the observations in the lowest energy bins. Subsequently, the residual is fitted with a one point plasma emission as for the other objects. The second row of each object is a Raymond–Smith fit with a very large absorption column density $N_H = 10^{22}$ cm^{-2}. In the rest of the paper we will adopt the figures given in Table 3. But the uncertainty has to be kept in mind.

The X-ray luminosities scatter over a large range from 0.0002 $L_\odot$ to 0.4 $L_\odot$. The question is to what other properties of the system L_X may be related. Firstly, we note that the four most X-ray luminous objects are d-types, whereas the s-types are typically two orders of magnitude fainter.

We also find a strong correlation with the luminosity L^* of the hot binary component. The relation

$$L_{\text{plasma}} = 10^{-5} \times L^* \tag{2}$$

fits the data surprisingly well (cf. Fig. 5). We emphasize that the diagram contains additional parameters: As mentioned above, the upper points are d-types, the lower are s-types. The object in the lower left corner (EG And) which makes the correlation obvious is the only object in the plot that is not a symbiotic nova.

For the β-type emission, the energy source for the X-ray emission is basically the kinetic energy of the wind from the hot star. The question is: what fraction of the available energy is converted into X-rays? This efficiency may be one of the observational figures that can serve as a test for hydrodynamical models. Unfortunately, the winds from the hot stars are difficult to observe. Even their existence is clarified only in a few cases. Sophisticated analyses of wind line profiles are available only for two objects, namely AG Peg (Schmutz 1996) and EG And (Schmutz et al., in preparation). A further object, SMC 3 (Jordan et al. 1996) yields only an upper limit, because the plasma component is not detected.

In Table 6 we collect the relevant characteristics. They are compatible with equal conversion efficiency for AG Peg and EG And, although the systems are rather different. If this is a general rule, relation (2) indicates that the kinetic energy of the winds of the hot stars in symbiotic binaries is proportional to their luminosity.

4.4. Plasma temperature

The characteristic plasma temperatures range from $3 \cdot 10^6$ K to $15 \cdot 10^6$ K. An upper limit for the plasma temperature in the shock can be derived from the velocity v_∞ of the hot wind: The thermal energy per particle can not exceed the kinetic energy per particle in the wind, hence

$$3kT_{\text{Plasma}} < \frac{1}{2} m_H v_\infty^2 \ . \tag{3}$$

With the velocities quoted in Table 6 we find that this limit is reached in EG And whereas our temperature for AG Peg stays below. In fact, models predict that the hottest region has only a small emission measure, and that the shocked gas rapidly cools through more or less adiabatic expansion (Walder, personal communication).

4.5. The symbiotic novae

Symbiotic novae (Allen 1980) are a small subgroup (eight generally accepted objects) of the symbiotic stars. They undergo large amplitude (up to $\Delta V \approx 7^m$) outbursts of long duration (several decades). The basic nature of the outbursts is probably

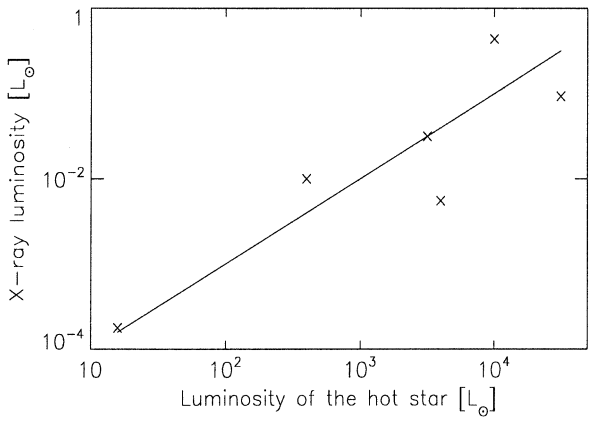

Fig. 5. X-ray luminosity (this Paper) versus the luminosity of the hot star (taken from Mürset et al. 1991, Mürset & Nussbaumer 1994, and Jordan et al. 1994). Unfortunately, no reliable value for the luminosity of RX Pup is available. The solid line corresponds to $L_X = 10^{-5} \times L^*$.

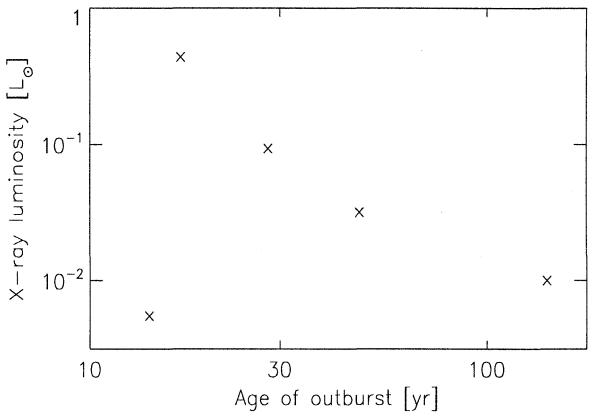

Fig. 6. X-ray luminosity versus the age of the outburst for symbiotic novae.

similar to classical novae, i.e. they are thermo-nuclear events in a hydrogen-rich layer accreted on top of the surface of the white dwarf. We have to discuss two issues: the X-ray brightness of symbiotic novae in general, and the X-ray evolution in the course of the outburst.

- From the detection statistics (Table 5) we conclude that among symbiotic stars the symbiotic novae are conspicuously X-ray bright. The EINSTEIN observatory was pointed to three symbiotic novae, and all of them were detected, whereas all of the 15 other observed symbiotics were too weak (Allen 1981). Six of the eight symbiotic systems were covered by pointed PSPC observations – and, again, *all* of them are detected. We note that the symbiotic novae have neither smaller distances nor smaller extinctions than average symbiotics.
  We suggest that the particular X-ray brightness is simply a consequence of the fact that the average luminosities of symbiotic novae (see Mürset & Nussbaumer 1994 and Jordan et al. 1996) are higher than for other symbiotic stars (Table 5 of Mürset et al. 1991; see also Fig. 7 of Mürset et al. 1996a). For the α-types (RR Tel and SMC 3) the relation between stellar luminosity and X-ray brightness is obvious; even more important is the high temperature of these objects. For the β-types the X-ray brightness also scales with the hot star's luminosity (Sect. 4.3).
- The three EINSTEIN count rates led Allen (1981) and Kwok & Leahy (1984) to suggest that the X-ray luminosity of symbiotic novae is declining with time. Hoard et al. (1996) add ROSAT count rates of RR Tel, AG Peg, and PU Vul that apparently confirm this picture. However, there are some problems with the plot of Hoard et al:
  - ROSAT data and published EINSTEIN data are mixed together which cannot be done independently of a theoretical model due to the different energy dependent sensitivities.
  - Hoard et al. determine the distance of PU Vul by adopting the same maximum brightness for RR Tel and PU Vul. We do not see any physical explanation for this assumption.
  - Hoard et al., as well as the earlier authors compare photospheric emission (RR Tel) and the emission of a hot shocked gas (e.g. AG Peg), which are completely different physical phenomena.

Fig. 6 shows the plasma luminosity of symbiotic novae as a function of the time since the beginning of the outburst. Our plot includes only data that were derived from ROSAT observations of hot gas emission by fitting these observations with a model. The distances are homogeneously derived from the brightness of the cool component. We find that the relation claimed by Hoard et al. still holds, qualitatively, for AG Peg, RR Tel, V1016 Cyg, and HM Sge, but PU Vul is far below the required luminosity. The figure would look similar if the luminosities of the hot star were displayed.

4.6. CH Cyg

X-rays from CH Cyg were detected first with EXOSAT (Leahy & Taylor 1987). ROSAT observations have been published by Leahy & Volk (1995). The pulse height distribution (Fig. 3) peaks at $h\nu \approx 0.85$ keV, however, it looks somewhat different than the other β-types, with a flat top and a wing extending to high energies. Like Leahy & Volk (1995), we were not able to fit the pulse hight distribution of CH Cyg with a one point model. The best "fit" to the soft part ($h\nu \leq 0.9$ keV) is shown in Fig. 3: $T_{\rm Plasma} = 0.3$ keV, $L_{\rm Plasma} = 0.006$ L$_\odot$. The residual can be considered as a γ-type component. Leahy & Volk fitted the observations by adding a power law component. Since we do not see an obvious physical explanation for power law emission we do not advocate such a model. We prefer to remain without a solution. Other peculiarities are reported for CH Cyg, and one of them may be the reason for the hard emission wing.

4.7. The γ-types: GX1+4 and Hen 1591

The pulse height distribution of Hen 1591 is within the (large) uncertainty identical with that of GX1+4. Little is known about Hen 1591. We can only speculate that its X-ray similarity to GX1+4 might be a hint that Hen 1591 contains an accreting neutron star as GX1+4 (Davidsen et al. 1977).

Acknowledgements. We thank Tim Freyer, Harry Nussbaumer, and Hans Martin Schmid whose comments helped to improve this Paper. Work on ROSAT data in Kiel is supported by DARA grant 50 OR 94091 and 50 OR 96173

References

Allen D.A., 1980, MNRAS 190, 75
Allen D.A., 1981, MNRAS 197, 739
Allen D.A., 1984, Proc. ASA 5, 369
Allen D.A., Wright A.E., 1988, MNRAS 232, 683
Anderson C.M., Cassinelli J.P., Sanders W.T., 1981, ApJ 247, L127
Bickert K.F., Greiner J., Stencel R.E., 1996, in: Supersoft X-ray Sources, ed. J. Greiner, Lecture Notes in Physics 472, Springer
Davidsen A., Malina R., Bowyer S., 1977, ApJ 211, 866
Dopita M.A., Ford H.C., Webster B.L., 1985, ApJ 297, 593
Downes R.A., Keyes C.D., 1988, AJ 96, 777
Fernie J.D., 1985, PASP 97, 653
Girard T., Willson L.A., 1987, A&A 183, 247
Greiner J., Bickert K., Luthardt R. et al., 1996, submitted to A&A
Greenhill J.G., Sharma D.P., Dieters S.W.B., Sood R.K., Waldron L., Storey M.C., 1993, MNRAS 260, 21
Groenewegen M.A.T., Lamers H.J.G.L. 1989, A&AS , 79, 359
Hinkle K.H., Fekel F.C., Johnson D.S., Scharlach W.W., 1993, AJ 105, 1074
Hoard D.W., Wallerstein G., Willson L.A., 1996, PASP 108, 81
Ivison R.J., Seaquist E.R., 1994, MNRAS 268, 561
Jordan S., Mürset U., Werner K., 1994, A&A 283, 475
Jordan S., Schmutz W., Wolff B. et al., 1996 A&A, in press
Kahabka P., Pietsch W., Hasinger G., 1994, A&A 288, 538
Kenyon S.J., Fernández-Castro T., Stencel R.E., 1988, AJ 95, 1817
Kwok S., Leahy D.A., 1984, ApJ 283, 675
Kwok S., Bignell R.C., Purton C.R., 1984, ApJ 279, 188
Leahy D.A., Taylor A.R., 1987, A&A 176, 262
Leahy D.A., Volk K., 1995, ApJ 440, 847
Meatheringham S.J., Dopita M.A., 1991, ApJS 75, 407
Michalitsianos A.G., Maran S.P., Oliversen R.J. et al., 1991, ApJ 371, 761
Morgan D.H., 1996, MNRAS 279, 301
Morrison R., McCammon D., 1983, ApJ 270, 119
Munari U., Renzini A., 1992, ApJ 397, L87
Munari U., Whitelock P.A., 1989, MNRAS 237, 45p
Mürset U., Nussbaumer H., 1994, A&A 282, 586
Mürset U., Nussbaumer H., Schmid H.M., Vogel M., 1991, A&A 248, 458
Mürset U., Jordan S., Walder R., 1995, A&A 297, L87
Mürset U., Schild H., Vogel M., 1996a, A&A 307, 516
Mürset U., Jordan S., Wolff B., 1996b, proceedings of the workshop on supersoft X-ray sources held in Garching from Feb. 28 to March 1, 1996, Springer (Paper I)
Nussbaumer H., Vogel M., 1987, A&A 182, 51
Nussbaumer H., Vogel M., 1996, A&A 307, 470
Nussbaumer H., Walder R., 1993, A&A 278. 209
Nussbaumer H., Schmutz W., Vogel M., 1995, A&A 293, L13
Orio M., 1993, A&A 274, L41
Penston M.V., Allen D.A., 1985, MNRAS 212, 939
Predehl P., Friedrich S., Staubert R., 1995, A&A 294, L33
Piro L., Cassatella A., Spinoglio L., Viotti R., Altamore A., 1985, IAU Circ. No. 4082
Raymond J.C., Smith B., 1977, ApJS 35, 419
Rebeirot E., Azzopardi M., Westerlund B.B., 1993, A&AS 97, 603
Schild H., 1989, MNRAS 240, 63
Schmutz W., 1996, in: Science with the Hubble Space Telescope II, eds. P. Benvenuti, F.D. Macchetto, E.J. Schreier
Seaquist E.R., Taylor A.R., Button S., 1984, ApJ 284, 202
Taranova O.G., Yudin B.F., 1983, A&A 117, 209
Taylor A.R., Seaquist E.R., 1984, ApJ 286, 263
Thackeray A.D., Webster B.L., 1974, MNRAS 168, 101
Viotti R., Piro L., Friedjung M., Cassatella A., 1987, ApJ 319, L7
Viotti R., Giommi P., Friedjung M., Altamore A., 1995, in Cataclysmic Variables, eds. A. Bianchini, M. Della Valle, and M. Orio, Kluwer, p. 195
Vogel M., 1991, A&A 249, 173
Vogel M., 1993, A&A 274, L21
Vogel M., Nussbaumer H., 1992, A&A 259, 525
Vogel M., Nussbaumer H., Monier R., 1992, A&A 260, 156
Vogel M., Nussbaumer H., 1994, A&A 284, 155
Walder R., 1995a, in: Asymmetrical Planetary Nebulae, eds. A. Harpaz, N. Soker, Ann. Israel Phys. Soc. 11, 248
Walder R., 1995b, in: Wolf-Rayet stars: binaries, colliding winds, evolution, eds. K.A. van der Hucht and P.M. Williams, IAU Symp. 163, p. 420
Walder R., Vogel M., 1993, in: Cataclysmic Variables and Related Objects, eds. O. Regev, G. Shaviv, Ann. Israel Phys. Soc. 10, 331
Wallerstein G., Willson L.A., Salzer J., Brugel E., 1984, A&A 133, 137
Webster B.L., Allen D.A., 1975, MNRAS 171, 171
Whitelock P.A., Catchpole R.M., Feast M.W. et al., Carter B.S., 1983, MNRAS 203, 363
Willson L.A., Wallerstein G., Brugel E.W. et al., 1984, A&A 133, 154
Zimmermann H.U., Becker W., Belloni T. et al., 1994, EXSAS User's Guide, MPE Report 257

This article was processed by the author using Springer-Verlag LaTeX A&A style file *L-AA* version 3.